International Journal of Physics and Applications

E-ISSN: 2664-7583
P-ISSN: 2664-7575
IJOS 2023; 5(1): 82-87

www.physicsjournal.in
Received: 03-01-2023
Accepted: 16-02-2023

Kasala Suresha
Department of Physics,
Government First Grade College,
MCC 'B' Block, Davanagere,
Karnataka, India

Corresponding Author:
Kasala Suresha
Department of Physics,
Government First Grade College,
MCC 'B' Block, Davanagere,
Karnataka, India

Electron energy relaxation in SiGe quantum wells

Kasala Suresha

DOI: https://doi.org/10.33545/26647575.2023.v5.i1b.65

Abstract
In this article, we theoretically calculated the hot electron energy relaxation induced by longitudinal acoustic (LA) phonons, longitudinal optical (LO) phonons and importantly two-transverse acoustic (2TA) phonons in two-dimensional SiGe quantum wells, by incorporating dynamic screening effect in LA phonon scattering and hot-phonon effect in LO phonon scattering mechanisms. At the low-temperature regime, the ELR is found to be dominated by LA phonons and at higher temperature ELR is dominated by LO phonons. In the intermediate temperature range, 2TA phonon scattering mechanism is very important and we incorporated in our calculations. The unscreened longitudinal acoustic (LA) phonon due to deformation potential (DP) coupling is dominant over the screened acoustic piezoelectric phonon contribution. At higher temperatures, there is a crossover from ELR due to LA phonons to ELR due to longitudinal optical (LO) phonons with the cross-over temperature being about Te∼40K. The LA phonon screening effect and hot phonon effect is demonstrated to reduce ELR significantly. In the intermediate temperature range (30 K< T_e < 90 K), 2TA phonon scattering mechanism is found to be dominating.

Keywords: Transverse acoustic phonons, acoustic and optical phonons, electron energy relaxation, SiGe, quantum well

1. Introduction
Hot carrier transport has been an important issue in both electronic and optoelectronic devices and energy relaxation is one of the most significant factors in hot carrier transport. Theoretical and experimental studies of hot carrier relaxation have primarily focused on electrons in direct gap materials such as GaAs [1-6]. During last two decades, a big progress has been made in studying the behavior of strongly correlated electrons confined in two-dimensional (2D) quantum wells. The metal-insulator transition, discovered initially in low-disorder silicon metal-oxide-semiconductor field effect transistors (MOSFETs) and subsequently observed in many other strongly correlated two-dimensional systems [7], has attracted a great deal of attention and is still not completely understood [8]. It is generally agreed that for the zero-magnetic-field metallic state to exist in 2D, strong interactions between carriers are needed. Other effects of strong correlations include greatly enhanced spin susceptibility [9] and the effective mass [10]. The 2D electron system in silicon turned out to be a very convenient object for studies of the strongly correlated regime due to relatively high effective band mass (0.19 m_e compared to 0.067 m_e in n-type GaAs/AlGaAs heterostructures and the existence of two almost degenerate valleys in the spectrum (n_v = 2), which further enhances the correlation effects [11]. However, even in the highest quality Si MOSFETs, the maximum electron mobility did not exceed 3 m^2/Vs, and the effects of the residual disorder mask the effects of interactions on the insulating side of the metal-insulator transition, where the formation of the Wigner crystal is expected. This calls for a new high-mobility silicon-based 2D system to be developed.
The study of scattering mechanisms in 2DEGs is a mature field of research where a tremendous amount of work has been performed. A common approach to experimentally determine the dominant scattering mechanisms in two-dimensional systems is to extract the power-law exponent from the density dependence of the mobility. Several experimental and theoretical studies have used similar techniques to analyze disorder in GaAs/AlGaAs structures [12], Si MOSFETs, [13] and doped [14] and un-doped [15] Si/SiGe heterostructures. With this in mind, we present in this work a systematic study of the temperature dependence of electron energy loss rate for different scattering mechanisms in SiGe quantum wells with well

width 50 nm.

The interaction of electrons with phonons plays an important role in determining the behavior of electrons under high electric field. One of such is electron energy loss rates (ELR) which provide better understanding of electron-phonon interaction than conventional mobility studies. Most of the experimental observations and theoretical analysis of ELR studies have been focused on GaAs, GaInAs, InSb and GaSb systems because of the favorable energy gap and well developed crystal growth techniques. Group III nitride materials are very suitable for applications in high power, high frequency and high temperature electronics [16]. Most devices are designed to operate under high electric field. At a high electric field, the electrons equilibrate at a much higher temperature than the lattice temperature. The determination of the temperature of electrons under electric field heating conditions in the steady sate provides useful information about electron-phonon interactions involved in the energy relaxation process. Till recently, very little work appears in literature concerning the study of ELR in widely band gap III nitride semiconductor such as GaN/AlGaN when 2D electron gas is confined in other semiconductors. GaN has vast applications in optoelectronic and electronic device technologies. GaN has recognized as very promising material for the visible ultraviolet range. Light Emitting Diodes (LEDs) and Laser Diodes (LDs) have been developed and show potential applications [17, 18]. The aim of this work is to show, the importance of incorporating electron-two-phonon scattering mechanism in the energy loss rate studies in 2D SiGe quantum well. In bulk and 2D semiconductor heterostructure, it is established that the effect due to two-phonon interaction are observable and have significant influence on the transport properties. To explain the energy loss data in SiGe quantum well, calculations are presented by taking into account this additional scattering mechanism. The experimental results for energy loss rate in SiGe quantum wells are awaiting to compare our theoretical results.

2. Theory

The theoretical purpose of our calculation is a quantum well formed in SiGe/Si heterostructure. In our calculations, we assumed that electron transitions occur within the first size-quantization sub-band. In the one-phonon process, the momentum and energy conservation requirement prevents the more energetic acoustic phonons from scattering electrons. If and $\boldsymbol{q}$ and $\boldsymbol{q}'$ are the phonon wave vector in the short wavelength regions such that $\boldsymbol{Q} = \boldsymbol{q} + \boldsymbol{q}'$ is quite small so as to lie in the long wavelength region. Further, it will be assumed that the electrons are quasi-2D, with the electron wave function given by

$$\Psi_{\boldsymbol{k}}(\boldsymbol{r}) = \frac{1}{\sqrt{A}} e^{i\boldsymbol{k}*\boldsymbol{r}} \Phi(z) \tag{1}$$

where A is the area in the plane of the layer, $\boldsymbol{k}$ and $\boldsymbol{r}$ are the usual two-dimensional vectors. Here only the first subband is assumed to be occupied.

It is convenient to calculate average energy loss per electron by calculating the energy gained by phonons from the electrons and dividing by the number of electrons (N_e) participate [9]

$$\langle P \rangle = -\frac{1}{N_e} \sum_{\boldsymbol{k},\boldsymbol{q},\boldsymbol{q}'} \hbar(w_q + w_{q'}) \frac{2\pi}{\hbar} \{(N_q + 1)(N_{q'} + 1) f(E_{k'})[1 - f(E_k)] - N_q N_{q'} f(E_k)[1 - f(E_{k'})]\} |M(\boldsymbol{q},\boldsymbol{q}')|^2 \left|F(\boldsymbol{q}_z,\boldsymbol{q}_{z'})\right|^2 \delta(E_{k'} - E_k - \hbar(w_q + w_{q'}))$$

with $f(E_k)$ and N_q respectively representing the Fermi distribution with T_e and Bose distribution with T_L. $\left|F(\boldsymbol{q}_z,\boldsymbol{q}_{z'})\right|^2$ is the overlap integral.

2.1 Two-phonon processes

In the one-phonon process, the momentum and energy conservation requirement prevents the more energetic acoustic phonons from scattering electrons. However, in two-phonon process the additional phonon adds an extra degree of freedom and allows the acoustic phonon having energies greater than those permitted in one-phonon transitions to participate in the scattering of electrons. If and **q** and **q'** are the phonon wave vector in the short wavelength regions such that $\boldsymbol{Q} = \boldsymbol{q} + \boldsymbol{q}'$ is quite small so as to lie in the long wavelength region, then the two-phonon process can be treated formally as one-phonon process. The effective two-phonon interaction Hamiltonian for bulk semiconductor was mentioned detail in [19]. The contribution to the electron ELR in quantum well and heterojunction system for the two-phonon process can be calculated by employing the bulk description of phonons.

In bulk semiconductors there exist in literature, a strong experimental evidence supported by theoretical analysis for the two-phonon processes [19 and references therein]. Sandercock [20] was the first to suggest the importance of two-phonon processes from the study of I-V characteristics of high purity InSb and pointed out that two-phonon processes can explain the missing energy loss rate. A fair good agreement is obtained between experimental and theoretical energy loss rate in n-InSb in the electron temperature range 10-20K by considering 2TA phonons with one adjustable parameter-the 2TA scattering rate [18]. Similar good results have been obtained in bulk GaAs and GaSb in the intermediate temperature range [21].

In 2D semiconductors, for GaAs/GaAlAs quantum wells, in comparison between experimental data and theoretical observation, it was found that below 20K the dominant source of energy relaxation is by acoustic phonon emission and above 40K the LO phonons dominates the energy loss process. Electron-2TA phonon interaction has significant influence on the energy loss rate in the intermediate temperature range 20-40K [19]. In GaInAs/AlInAs heterojunctions, the ELR by 2TA phonons is significant in the

intermediate temperature range 20-40K, also theoretical calculations for ELR have been studied for GaSb and InSb quantum wells by considering 2TA phonons [22]. Without incorporating 2TA phonons, no good agreement is obtained for ELR between experimental and theoretical data over the wide temperature range.

It is demonstrated that, investigation of Gruneisen parameters and the phonon spectra in GaN indicating low-frequency phonon vibration modes correspond to change of thermal expansion. Below 5THz, the significant weighted negative values of more Gruneisen parameters, caused by the weakening of mixing mode constituted with two-transverse acoustic (2TA) modes [23]. Second order transverse acoustic (2TA) phonon mode at 300cm^{-1} was observed on Si substrate from Raman spectra of CdSe quantum dots [24]. In Zinc nanowires, some overtones due to 2TA phonon peaks are observed at high temperature due to larger wave vector from Raman scattering study [25].

It is convenient to calculate average energy loss per electron by calculating the energy gained by phonons from the electrons and dividing by the number of electrons (N_e) participate

$$\langle P\rangle = -\frac{1}{N_e}\sum_{k,q,q'}\hbar(w_q + w_{q'})\frac{2\pi}{\hbar}\{(N_q+1)(N_{q'}+1)f(E_{k'})[1-f(E_k)] - N_qN_{q'}f(E_k)[1-f(E_{k'})]\}|M(q,q')|^2\left|F(q_z,q_{z'})\right|^2\delta(E_{k'}-E_k-\hbar(w_q+w_{q'})) \quad (3)$$

with $f(E_k)$ and N_q respectively representing the Fermi distribution with T_e and Bose distribution with T_L. $\left|F(q_z,q_{z'})\right|^2$ is the overlap integral. The electron-two-phonon matrix element restricting to transverse acoustic branch of phonons is given by

$$|M(q,q')|^2 = \left(\frac{\hbar D\, p_{\Xi}^{1/2}}{2\rho\Omega\, a^2 (w_q w_{q'})^{1/2}}\right) \quad (4)$$

By evaluating equation (2) using equation (3) the average electron ELR yields,

$$\langle P\rangle_{2TA} = \frac{m^{*2}D_{\Xi}^2 p_{\Xi}}{N_s\pi^2\hbar\rho^2 a^7}\left(\frac{T_e}{\theta_{TA}}\right)\left[\exp\left(\frac{\theta_{TA}}{T_L}\right)-1\right]^{-2}\frac{\left[exp\left\{2\theta_{TA}\left(\frac{1}{T_L}-\frac{1}{T_e}\right)\right\}-1\right]}{\left[1-exp\left(-\frac{2\theta_{TA}}{L}\right)\right]}\left[ln(1+exp\{\eta\}) - ln\left(1+exp\left\{\eta-\frac{2\theta_{TA}}{T_e}\right\}\right)\right]\int_{-\infty}^{\infty}|F(q_Z)|^2 dq_Z \quad (5)$$

where $\eta = \frac{E_f}{k_B T_e}$, $\theta_{TA} = \left(\frac{\hbar w_{\Xi}}{k_B}\right)$, $\hbar w_{\Xi}$ is 2TA phonon energy, a is lattice constant, and N_s is the carrier concentration. E_f is the Fermi energy which is given by $E_f = k_B T_e ln\left[exp\left(\frac{E_F}{k_B T_e}\right)-1\right]$ with $E_F = \frac{\pi\hbar^2 N_s}{m^*}$. The overlap integral for quantum well is $|F(q_z)|^2 = \left[\frac{sin\left(\frac{Lq_z}{2}\right)}{\left(\frac{Lq_z}{2}\right)}\frac{1}{1-\left(\frac{Lq_z}{2\pi}\right)^2}\right]^2$.

2.2 Electron-acoustic deformation potential scattering

Following the subband procedure and assuming the phonon modes to be the same as those of bulk semiconductors, one can calculate the expression for the energy loss rate for screened acoustic deformation potential, piezoelectric scattering for the average electron energy loss rate due to screened acoustic deformation potential scattering can be expressed as

$$\langle P\rangle_{DP} = \frac{E_d^2 m^* k_F}{4N_s\pi^2\rho\hbar}\int_0^{\infty}\int_0^{\infty} q^2 S^2(q_{\parallel})\, F_1(\boldsymbol{q})\, \gamma(\eta_-,\eta_+)dq_{\parallel}dq_z \quad (6)$$

where $F_1(\boldsymbol{q}) = |F(q_z)|^2\left[exp\left\{\frac{\hbar\omega_q}{k_B}\left(\frac{1}{T_L}-\frac{1}{T_e}\right)\right\}-1\right]N_q$

and $\gamma(\eta_-,\eta_+) = \int_0^{\infty}\frac{1}{\sqrt{X}}f(X+\eta_-^2)\left[1+f(X+\eta_+^2-\mu)\right]dX$

where $f(X+\eta_{\pm}^2) = \frac{1}{[exp\{\xi(X+\eta_{\pm}^2)\}+1]}$

with $\eta_{\pm}^2 = \left(\frac{q_{\parallel}}{2k_F}\pm\frac{m^*\omega_q}{\hbar k_F q_{\parallel}}\right)^2$, and $\xi = \frac{E_F}{k_B T_e}$ and $\mu = \frac{E_f}{E_F}$ with $E_f = k_B T_e\ \ln\left[\exp\left(\frac{E_F}{k_B T_e}\right)-1\right]$, where Fermi energy, $E_F = \left(\frac{\pi\hbar^2 N_s}{m^*}\right)$

The screening function, $S^2(q_\parallel) = \left[1 + \frac{q_s}{q_\parallel} H(q_\parallel)\right]^{-2}$ with screening parameter, $q_s = \left(\frac{2m^* e^2}{\varepsilon_s \hbar^2}\right)$.

The screening form factor, $H(q_\parallel) = \frac{b\,(8b^2+9b\,q_\parallel+3q^2)}{8(b+q_\parallel)^3}$ for heterojunction and

$H(q_\parallel) = \frac{4}{4\pi^2+L^2 q_\parallel{}^2}\left[\frac{3}{4}Lq_\parallel + \frac{2\pi^2}{Lq_\parallel} - \frac{8\pi^4(1-e^{-Lq_\parallel})}{L^2 q_\parallel{}^2(4\pi^2+L^2 q_\parallel{}^2)}\right]$ for Quantum Wells.

2.3 Electron-acoustic piezoelectric potential scattering:

Similarly, the average electron energy loss rate for screened acoustic piezoelectric scattering

$$\langle P\rangle_{PZ} = \frac{(eh_{14})^2 m^* k_F}{4N_s\pi^2\rho\hbar}\int_0^\infty\int_0^\infty A_i S^2(q_\parallel) F_1(\boldsymbol{q})\,\gamma(\eta_-,\eta_+)dq_\parallel dq_z \tag{7}$$

where A_i for longitudinal piezoelectric scattering is given by $A_l = \left(\frac{9q_\parallel{}^4 q_z^2}{2q^6}\right)$ and for transverse piezoelectric scattering $A_t = \left(\frac{8q_\parallel{}^2 q_z^4 + q_\parallel{}^6}{2q^6}\right)$. h_{14} is the piezoelectric coupling constant.

2.4 Electron-longitudinal optical phonon potential scattering

Including the hot-phonon effect, the average energy loss rate due to longitudinal optical (LO) phonon scattering can be expressed as

$$\langle P\rangle_{LO} = \frac{(\hbar w_o)^2 m^* k_F e^2}{N_s\pi^2\hbar^3\varepsilon'}\int_0^\infty\int_0^\infty q^{-2}\,F(w_o,q_z)\,\gamma(\eta_-,\eta_+)\,dq_{||}dq_z \tag{8}$$

Where $\gamma(\eta_-,\eta_+) = \int_0^\infty \frac{1}{\sqrt{X}}\,f(X+\eta_-^2)[1-f(X+\eta_+^2)]\,dX$

with $f(X+\eta_\pm^2) = \left[exp\{\xi\,(X+\eta_\pm^2-\mu)\}+1\right]^{-1}$; $\eta_\pm^2 = \left(\frac{q_{||}}{2k_F} \pm \frac{m^* w_q}{\hbar k_F\, q_{||}}\right)^2$; $\xi = \frac{E_F}{k_B T_e}$; $\mu = \frac{E_f}{E_F}$

and $F(w_o,q_z) = |F(q_z)|^2\left[N_q^{HP}\left(exp\left\{-\frac{\hbar w_o}{k_B T_e}\right\}-1\right) + \left(exp\left\{-\frac{\hbar w_o}{k_B T_e}\right\}\right)\right]$

here N_q^{HP} is the non-equilibrium distribution function of phonons given by

$$N_q^{HP} = \left[\frac{N_q + \tau_p\,\alpha\left(exp\left\{-\frac{\hbar w_o}{k_B T_e}\right\}\right)}{1+\tau_p\,\alpha\left(1-exp\left\{-\frac{\hbar w_o}{k_B T_e}\right\}\right)}\right] \tag{9}$$

with τ_p be the optical phonon life time and α is given by

$$\alpha = \frac{2m^* k_F e^2(\hbar w_o)}{\hbar^3 L\varepsilon' q_{||} q^2}\,|F(q_z)|^2\,\gamma(\eta_-,\eta_+) \tag{10}$$

with $\varepsilon' = \left(\frac{1}{\varepsilon_\infty} - \frac{1}{\varepsilon_s}\right)^{-1}$

The total power loss per electron is obtained by adding contribution from LA deformation, piezoelectric, LO phonons and two-phonon scattering (equations 5, 6, 7 and 8).

3. Results and Discussion

Theoretical calculations of power loss per electron *P* as a function of electron temperature for acoustic phonons, longitudinal optical phonon and 2TA phonon processes have been performed for the SiGe/Si quantum well quantum wells. The material parameters used in calculations characteristic of SiGe are m^* = 0.92m_0, V_s =8.433x10^3 m/s, ρ = 2329 kg/m^3, $\hbar w_o$ = 50.0 meV, τ_p= 10.0 ps, ε_∞ = 7.45, ε_s = 11.7, D_Ξ = 10x10^3 eV, $\hbar w_\Xi$ = 40 meV and lattice constant a = 5.431A^0.

The above Figure 1 shows the contributions to average energy loss rate from acoustic deformation potential, acoustic piezoelectric, longitudinal optical phonon and 2TA phonon scattering mechanisms. In calculations we used carrier concentration N_s = 1.0x10^{13} m^{-2}, quantum well width L = 50 A^0, lattice temperature T_L = 3.0 K deformation potential constant E_d = 12.0 eV and h_{14} = 0.6x10^9 V/m. In the temperature region we considered here indicates that acoustic deformation potential scattering

mechanism is dominant mechanism compared to piezoelectric scattering mechanism which was earlier published by us previously [26]. The same dominant mechanism was also observed in 2D GaAs, GaInAs and GaN quantum wells [19, 22, 27]. In the acoustic deformation potential scattering mechanism, the only adjustable parameter is the deformation potential constant E_d. While calculating energy loss rate for LO phonon scattering, we assumed the optical phonon energy $\hbar w_o$ =50.0 meV, τ_p= 10.0 ps. The only adjustable parameter for LO phonon scattering mechanism is the optical phonon life time τ_p. Electron temperature T_e between 30 – 90 K, there is a need for new scattering mechanism as observed in GaAs, GaInAs and GaN quantum wells. Keeping in mind, we tried to incorporate new scattering mechanism such as electron – 2TA phonon interaction because in 2D semiconductors, for GaAs/GaAlAs quantum wells, in comparison between experimental data and theoretical observation, it was found that below 20K the dominant source of energy relaxation is by acoustic phonon emission and above 40K the LO phonons dominates the energy loss process. Electron-2TA phonon interaction has significant influence on the energy loss rate in the intermediate temperature range 20-40K [19]. In GaInAs/AlInAs heterojunctions, the ELR by 2TA phonons is significant in the intermediate temperature range 20-40K, also theoretical calculations for ELR have been studied for GaSb and InSb quantum wells by considering 2TA phonons [22]. Without incorporating 2TA phonons, no good agreement is obtained for ELR between experimental and theoretical data over the wide temperature range.

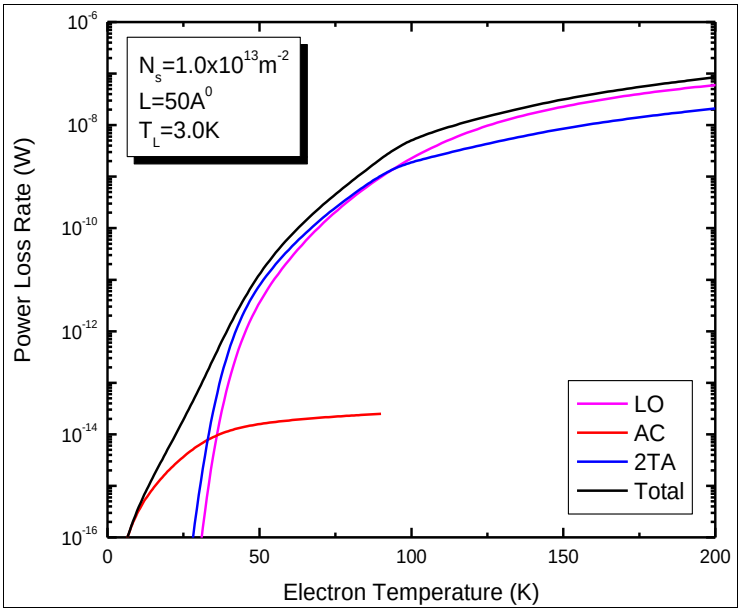

Fig 1: Electron energy loss rate as a function of electron temperature. The red line represents contribution due to acoustic phonon scattering, blue line for 2TA phonon scattering, pink line represents LO phonon scattering and black line for total contribution from all three scattering mechanisms

When the experimental observations are available for this SiGe quantum wells, these theoretical calculations will show good agreement with the observations. In considering 2TA scattering mechanism, we used 2TA deformation potential constant to be D_{Ξ} = 10x10^3 eV, and 2TA phonon energy to be $\hbar w_{\Xi}$ = 40 meV. In the figure red line shows the energy loss rate for acoustic phonon scattering (sum of acoustic deformation and piezoelectric). In both the scattering mechanisms, we used the dynamical screening effect as this screening effect will reduce the ELR significantly [19, 22]. The piezoelectric scattering mechanism is weak as compared to acoustic deformation potential scattering. The dominant scattering mechanism is due to the acoustic deformation potential in the lower temperature range (T_e <50 K). This study has already been published +. The pink line shows the contribution of ELR from LO phonon scattering with hot phonon effect, wherein we included hot phonon effect, as it reduces the ELR. The LO phonon scattering mechanism is dominant when the temperature is above 90 K. The blue line represents the electron-2TA scattering mechanism which is important dominant mechanism in the temperature range 30 – 90 K.

The importance of inclusion of 2TA phonon scattering in ELR is well explained in GaAs, GaInAs and GaN quantum wells. Our previous calculations in these quantum wells successfully explain with the experimental results [19, 22, 27]. As this new scattering mechanism is very important in the above materials, so we decided to include this new 2TA scattering mechanism in SiGe quantum well. Due to lack of availability of experimental results in SiGe, we just calculated all possible calculations. If the experimental data is available for SiGe quantum well, these calculations will help to compare the experimental results.

4. Conclusions

We included the new scattering mechanism such as electron-2TA phonon scattering mechanism in our calculations to calculate the average energy loss rate. This 2TA scattering mechanism is found to be important in satisfying the experimental results if the experimental data for SiGe quantum wells are available. In addition to this scattering mechanism, we also calculated the average energy loss rate for acoustic and longitudinal optical phonons. We included the screening mechanism in acoustic deformation potential scattering and hot phonon effect in LO phonon scattering as these effects will reduce the ELR considerably. We observed that acoustic phonons are dominating below 30K, longitudinal optical phonons are for above 90 K and in between 30 – 90K, the 2TA phonons are need to be considered as these are considered in GaAs, GaInAs and GaN quantum wells.

5. References

1. Sarma SD, Campos VB, Stroscio MA, Kim KW. Semicond. Sei. Technol. 1992;**7:**B60.
2. Cavicchia MA, Alfano RR. Phys. Rev. B 1993;48:5696.
3. Straw AJ, Vickers, Roberts JS. Semicond. Sei. Technol. 1992;**7**:B343.
4. Lutz J, Kuchar F, Ismail K, Nickel H, Schlapp W. Semicond. Sei. Technol. 1993;8:399.
5. Furuta T, Shigekawa N, Tomizawa M. Semicond. Sei. Technol. 1994;9:453.
6. Asmar NG, Markelz AG, Gwinn EG, Hopkins PF, Gossard AC. Semicond. Sei. Technol. 1994;9:828.
7. Abrahams E, Kravchenko SV, Sarachik MP. Rev. Mod. Phys. 2001;73:251.
8. Spivak B, Kravchenko SV, Kivelson SA, Gao XPA. Rev. Mod. Phys. 2010;82:1743.
9. Shashkin SV, Kravchenko VT, Dolgopolov, Klapwijk TM. Phys. Rev. Lett. 2001;87:086801.
10. Shashkin SV, Kravchenko VT, Dolgopolov, Klapwijk TM. Phys. Rev. B. 2002;66:073303.
11. Punnoose, Finkelstein AM. Science. 2005;310:289.
12. Laroche D, Das S, Sarma, Gervais G, Lilly MP, Reno JL. Appl. Phys. Lett. 2010;96:162112.
13. Chain K, hui Huang J, Duster JPK, Hu C. Semicond. Sci. Tech. 1997;12:355.
14. Dolgopolov V, Deviatov E, Shashkin A, Wieser U, Kunze U, Abstreiter G, *et al*., Superlattices Microst. 2003;33:271-278.
15. Mi X, Hazard TM, Payette C, Wang K, Zajac DM, Cady JV, *et al*, Phys. Rev. B. 2015;92:035304.
16. Morkoc H. Handbook of Nitride Semiconductors and Devices, Wiley-VCH, Heinheim, 2008;3.
17. Amano H, Kito M, Hiramatsn K, Akasaki I. J Appl. Phys. Part-2. 1989;28:L2112.
18. Nakamura S, Senoh M, Mukai T. Appl. Phys. Lett. 1993;62:2390.
19. Kubakaddi SS, Kasala Suresha, Mulimani BG. Semicond. Sci. Technol. 2002;17:557.
20. Sandercock JR. Solid State Comm. 1969;7:721.
21. Senda K, Simamoe K, Hamaguchi C. J Phys. C, Solid State Phys. 1980;13:1043.
22. Kubakaddi SS, Kasala Suresha, Mulimani BG. Physica E. 2003;18:475.
23. Li-Chun Xu, Ru-Zhi Wang, Xiaodong Yang, Hu Yan. JAP. 2011;110:043528.
24. Sheremet E, Duda A, Gridchin VA, Dzhagan VM, Hietschold M, Zahn DRT. Phys. Chem. Chem. Phys. 2015;17:21199.
25. Shi L, Wang C, Wang J, Fang Z, Xing H. Advances in Materials Physics and Chemistry. 2016;6:305.
26. Kasala Suresha. Int. J Adv. Res. Sci. & Comm. Technol. 2023;3:01.
27. Kasala Suresha, Int. J Res. Appl. Sci & Engg. Technol. 2022;10:IV.